



Effect of surface coating on droplet generation in flow-focusing microchannels

Bryan Palogan¹ · Ranganathan Kumar¹ · Samik Bhattacharya¹

Received: 24 May 2020 / Accepted: 9 August 2020 / Published online: 19 August 2020
© Springer-Verlag GmbH Germany, part of Springer Nature 2020

Abstract

Different stages of droplet generation are reported in this paper with two immiscible liquids, silicone oil and deionized water, inside a flow-focusing device for hydrophobic and hydrophilic channel walls. Hydrophobic and hydrophilic channels of identical geometry are compared. In this first set of experiments, the efficacy of the hydrophobic channel is compared with a square cross junction for a continuous oil phase with low viscosity. In the hydrophobic case, the flow-focusing design with a diverging outlet delays jetting and allows for the use of higher flow rate ratios in the squeezing regime. For the hydrophilic case, stable and well-structured droplet and slug generation can be achieved using oil and water, resulting in an inverse emulsion. However, the morphology of the fluid interface displays an unusual behavior compared to that of a hydrophobic microchannel. The droplet generation in the hydrophilic channel occurs following the formation of single and double T-junctions, a phenomenon hitherto unreported in the literature. The results demonstrate that the uncoated hydrophobic channels generate monodisperse droplets at a higher capillary number when compared to the hydrophilic channels.

Keywords Flow focusing · Hydrophobic · Hydrophilic · Droplet formation

1 Introduction

Over the past few decades, drop generation in microfluidics has been a prime area of research due to its wide array of chemical and biological applications. For instance, drops have been used for micro-mixing due to its low dispersion and rapid mixing (Tice 2003). The versatility and efficiency of microfluidic devices in generating monodisperse droplets have especially garnered attention in medical implementation. These characteristics make drops effective tools in applications such as clinical diagnostics and controlled drug delivery (Srinivasan et al. 2004; Kaler and Prakash 2014; Zhao 2013). Oil emulsions have various applications that range from food applications to pesticide creation (McClements and Decker 2000; Wang 2007).

Generally, droplets are generated when a dispersed phase is injected into an immiscible carrier fluid, or continuous phase. Shear stresses are imparted on the dispersed phase by the continuous phase until the interfacial tension is overcome and the drop is formed. Channel designs vary at the junction and take varying approaches in optimizing the interface interaction such that the production rate and monodispersity of droplets are maximized.

Numerous experimental papers have been published that investigate various geometries used in generating these emulsions (Gu et al. 2011; Zhu and Wang 2017). One such design is the T-junction, which consists of a primary channel that carries the continuous phase and an orthogonal channel that carries the dispersed phase (Nisisako et al. 2002; Glawdel et al. 2012; van Steijn et al. 2007; Wehking 2014). Flow-focusing (FF) devices are another type which can be subdivided into several categories. Axisymmetric FF devices have parallel continuous and dispersed phase flow, which is evenly pinched-off from all sides by the continuous phase (Serra 2007; Takeuchi 2005; Cramer et al. 2004).

A symmetric cross-junction consists of four rectangular channels with the same dimension; one inlet carrying the dispersed phase and two orthogonal continuous phase inlets which exit through one outlet (Edd 2008; Fu 2012; Van

✉ Samik Bhattacharya
samik.bhattacharya@ucf.edu

Bryan Palogan
bryanpa@Knights.ucf.edu

Ranganathan Kumar
Ranganathan.Kumar@ucf.edu

¹ Department of Mechanical and Aerospace Engineering,
University of Central Florida, Orlando, USA

Looet al. 2016). Introducing a smaller outlet, or orifice, into a symmetric FF device improves viscous shearing and increases the drop generation rate and monodispersity (Anna et al. 2003; Garstecki 2004; Nie 2008; Derzsi 2013). Other variations of FF geometry exist as well (Yobas 2006; Abate 2009). This study will focus on FF devices with an orifice. Aside from experimental results, many numerical studies have extensively explored these channel designs (Gupta et al. 2009; Gupta and Matharoo 2014; Nooranidoost 2019).

While the design of the fluid junction plays a significant role on the dynamics of the flow, other parameters are important to consider for droplet generation. Parameters such as fluid viscosity and channel aspect ratio have significant effects on the flow (Nie 2008; Gupta and Kumar 2010). Aside from axisymmetric devices, the wetting properties of a channel plays a crucial role on droplet generation. It has been demonstrated that the contact angle along the channel walls can be altered geometrically through microtexturing (Kim and Hidrovo 2012; Woolford et al. 2009). While this approach effectively controls channel hydrophobicity, design complexity is increased, making the manufacturing process more difficult.

Alternatively, channel hydrophobicity can also be altered through chemical processes that coat the walls with a material where the contact angle for the coating is known (Zhang 2013; Chiu 2014). Dreyfus has previously studied the importance of single-phase wetting for channel walls on the stability of flow patterns in a cross-junction; however, surfactants were used to vary the contact angles of the fluid (Dreyfus et al. 2003). It has been found that the use of surfactants can have a significant impact on the formation of drops (Glawdel and Ren 2012). Furthermore, it is common practice to utilize hydrophobic channels to generate an aqueous drop. Medical implementation of microfluidic devices is hindered by the hydrophobicity of the channel, as it results in the diffusion of material onto the channel walls (Mehta 2012). As such, it is beneficial to investigate the flow structures generated by partial wetting without the use of surfactants.

In this study, the droplet generation process and flow structures in two identical FF micro-channels with different wall coatings are compared. One channel has hydrophobic wall, whereas the other has hydrophilic wall coating. The objectives of this study are twofold: (1) compare the hydrophobic results for the FF device with those of a symmetric cross-junction and (2) investigate the effect of a hydrophilic surface coating on the drop generation process in the same polydimethylsiloxane (PDMS) channel.

2 Materials and methods

2.1 Experimental setup

Channels are manufactured by uFluidix following the procedures described by Chiu (2014). A PDMS polymer is cured on a SU-8 Master and bonded to a glass cover slide, which is coated with a PDMS layer, through oxygen plasma treatment. After bonding, the device is placed in an oven and baked in an oven at 95 °C to anneal the device and improve the bond between the surfaces. The microchannels are then coated with a polyacrylic acid coating, which renders the channel walls hydrophilic. For this study, both hydrophobic and hydrophilic channels are used. PDMS is inherently hydrophobic and the resulting contact angle of deionized (DI) water drops on the hydrophobic PDMS is about 100° whereas the contact angle for the chemically treated hydrophilic walls is about 55° (PP201, uFluidix, Canada).

To generate droplets using the FF device, two immiscible fluids are used in the channels. For this study, the inner fluid is DI water and the outer fluid is silicone oil with a kinematic viscosity of 5 cSt (Sigma-Aldrich, USA). A low-viscosity continuous phase was selected as many practical applications require the use of such fluids (Chan et al. 2016). Fluid interfacial tension and viscosities were measured in earlier studies using the pendant drop method and a Brookfield DVII + Pro viscometer (Wehking 2014; Yakhshi-Tafti et al. 2011).

The geometry of the FF design used in this study is shown in Fig. 1. The inlet width of the dispersed water phase and the continuous oil phase are 200 μm with an outlet orifice width of 100 μm. The orifice has a constant diverging angle of 5.7° and expands to the outlet width of 200 μm.

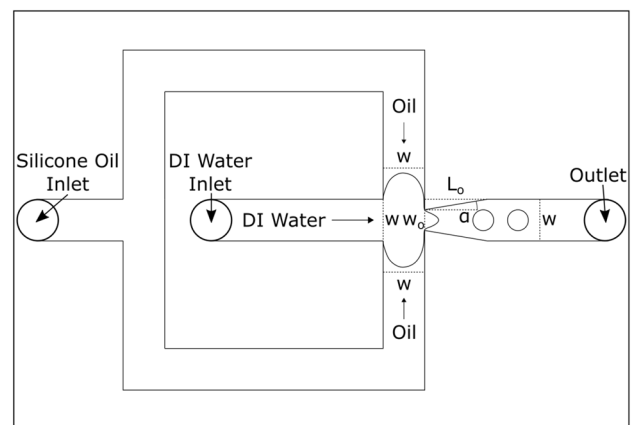


Fig. 1 Design of the microchannel. W is the initial channel width of 200 μm; W_o is the initial orifice width of 100 μm; α is the diverging angle of 5.7°; L_o is the length of the diverging region after the orifice, which is 500 μm. The channel height is 100 μm. Figure is not to scale

Droplet generation in a FF device occurs by pumping DI water through the central channel to the junction where it is pinched-off by the oil phase coming from the side channels. The fluid flow rates are controlled by two syringe pumps (KDS 210, KD Scientific, USA) and are injected into the system using polyethylene micro-tubing. The use of displacement pumping results in drop volume variation over time; however, it is still possible to achieve high rates of monodispersity with droplet size variation less than 5%, as found in the study by Wehking (2014). This is found to be the case in the periodic squeezing regime, which will be discussed in Sect. 3. Images of the channels are taken using a high-speed camera (i-Speed LT, Olympus, UK) attached to a microscope (Optiphot 100, Nikon, Japan) at a frame rate of 2000 fps. Drop images were processed and analyzed using MATLAB (MathWorks, USA).

The capillary number, $Ca = v_c \mu_c / \gamma$, is the ratio between the viscous forces and the interfacial tension, and thus an important parameter when considering the pinch-off during droplet generation. Here, v_c is the average velocity of the continuous phase, μ_c is the dynamic viscosity and γ is the interfacial tension, respectively. The ratio of the dispersed flow rate and continuous phase flow rate, Q_d/Q_c , is also an important parameter to identify as it relates the fluid flow rates.

Hydrophobic experiments are performed for DI water flow rate varying between 0.24 and 404 $\mu\text{L}/\text{min}$ and oil flow rates varying between 0.24 and 1213 $\mu\text{L}/\text{min}$. For hydrophobic testing, two different cases are considered. In the first case, the oil flow rate is held constant and the water flow rate is varied. These trials are repeated under different oil flow rates to determine the flow characteristics for different flow rate ratios at specified capillary numbers. The second case is similar to the first, but instead holds the DI water flow rate constant and varies the flow rate of the oil. Hydrophilic trials are performed for oil flow rates of 4 and 40 $\mu\text{L}/\text{min}$, and DI water flow rates varying between 4 and 1400 $\mu\text{L}/\text{min}$.

Experiments are initially run for a minimum of 30 min prior to recording data to allow the channels to reach a steady state. For this study, slugs are defined as segments of the dispersed phase with a maximum length that is larger than the channel width, whereas droplets have a maximum diameter smaller than the channel width.

PDMS channels are reusable; however, after many experimental tests, the channels degrade and must be replaced. Even so, with proper use, these channels can be reused for several experiments. At the end of an experiment, the channels are flushed with DI water and dried by pumping air through the channels.

3 Results and discussion

In this section, we first discuss drop generation in the hydrophobic channel followed by the same in the hydrophilic channel. Flow regimes for the hydrophobic case are compared with results for a symmetric cross-junction to identify the efficacy of the channel design. The hydrodynamic flow-focusing effect of the design's orifice improves the viscous shearing rate of the dispersed phase by accelerating the continuous fluid. It was shown by Tan et al. and Chen et al. that for a converging–diverging channel, a high velocity of the continuous phase liquid promotes the shear driven breakup of the dispersed phase (Tan et al. 2006; Chen et al. 2011). By immediately accelerating and decelerating the fluid through the diverging geometry, the velocity gradient can be maximized, resulting in greater shear stress that can improve droplet pinch-off. The results demonstrated that rapid production of monodisperse droplets could be achieved (Tan et al. 2006). The diverging structure of the orifice results in a variation of the capillary number along the length of the orifice. Capillary numbers are the largest for the inlet of the orifice as it has the smallest cross-sectional area, resulting in the greatest average continuous fluid velocity for the channel.

3.1 Droplet generation in hydrophobic channels

In the hydrophobic case, the dispersed phase, i.e., DI water, enters the cross-junction and forms an interface with the continuous phase, silicone oil. Various flow regimes were observed in this study and systematically plotted as functions of the flow rate ratio and continuous phase capillary number in Fig. 2 (Teo et al. 2019). Van Loo et al. performed a parametric sweep of a symmetric cross junction and the results are plotted in Fig. 2 to demonstrate the effects of the orifice and diverging channel on the regimes obtained (Van Loo et al. 2016).

The squeezing regime is characterized by a lag period in between drop generation and is divided into two categories: aperiodic and periodic, shown as phases (a) and (b) in Fig. 2. Periodic squeezing has a consistent average drop generation period within a specified threshold, whereas aperiodic squeezing is defined as squeezing for which the generation period is beyond the threshold and characterized by inconsistent drop size and spacing. Jetting, denoted by (c) in Fig. 2, occurs once the relaxation period between drops no longer exists and the dispersed fluid can no longer retract back to the junction after pinch-off. The continuous phase is no longer able to shear the droplets at the junction and drops are generated downstream from the orifice through Rayleigh–Plateau instabilities (Utada

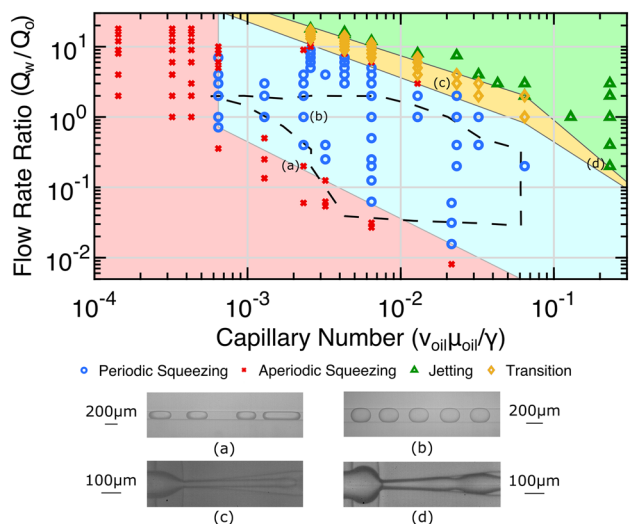


Fig. 2 Flow regimes for the hydrophobic channel walls plotted as a function of the flow rate ratio, Q_w/Q_o , and the capillary number of the continuous phase, Ca_{oil} . **a** Aperiodic squeezing regime, for which there is inconsistent droplet size and generation; **b** periodic squeezing regime, for which there is consistent droplet size and generation; **c** jetting regime; **d** transition from squeezing to jetting. The dashed line indicates the region for which periodic droplet generation was obtained by van Loo et al.

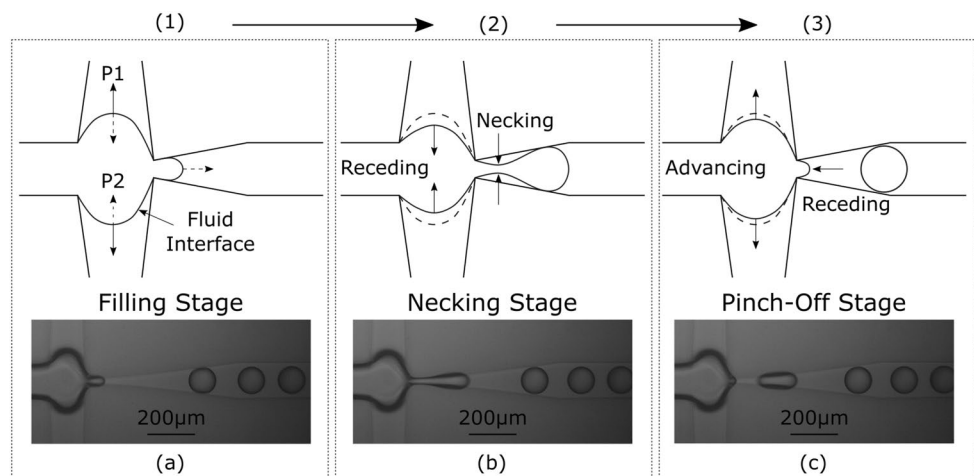
2007). Typically, drops produced in the jetting regime are slightly larger than the orifice width. Prior to jetting, an unstable transition zone exists between squeezing and jetting, denoted by the region (d) in Fig. 2.

The squeezing regime is characterized by the interface taking the shape of an inverse meniscus that encompasses majority of the fluid junction, as shown in Fig. 3. This inverse meniscus is attributed to the low-viscosity oil phase and pressure rise due to the constriction by the water phase at the orifice. Due to the low viscosity of the continuous phase, the viscous shearing force imparted on the dispersed phase is significantly reduced; allowing for the

formation of the meniscus structure that results in the re-circulation of the dispersed phase. In the squeezing regime, shown in Fig. 3, drops form at the junction with a ‘lag stage’ prior to the formation of the following drop (Glawdel et al. 2012). Initially after the pinch-off and separation of the previous drop, the dispersed phase attached to the bulk fluid at the junction retracts back towards the junction due to interfacial tension. During this relaxation period, the displacement of fluid back into the junction results in the re-circulation of the incoming dispersed phase. As a result, the meniscus interface moves away from the junction in the initial stages of filling, shown in Fig. 3a. The expansion continues until the constricted continuous phase causes the dispersed phase to recede. During the latter period of the filling stage, the drop diameter increases until the rapid formation of the neck, shown in Fig. 3b, which precedes the pinch-off of the drop. Immediately after the pinch-off, shown in Fig. 3c, the fluid attached to the bulk dispersed phase retracts back to the entrance of the orifice. Previous studies have demonstrated that using a more viscous continuous phase with a symmetrical cross-junction or flow-focusing design results in the necking once the dispersed phase is injected into the outlet.

The drop size is dependent upon the value of both the continuous oil, Q_o , and dispersed water, Q_w , flow rate. As such, D_{max}/w is plotted against the flow rate ratio in Fig. 4 to understand how the drop size scales with the fluid flow rates, as well as the length scale of the channel. Drop frequency is also plotted against the flow rate ratio in Fig. 5. For a constant, low oil flow rate, the water phase flow rate was varied. Increasing the DI water flow rate increases the flow rate ratio and it was found that the drop size and frequency increased with the water flow rate, as shown in Figs. 4 and 5. This is because as the thread is elongated laterally between the bulk fluid at the junction and the drop, the surface tension in the thread eventually acts to separate the generated drop and bulk fluid. By increasing the water flow rate, the time in which this critical length is achieved also reduced,

Fig. 3 Stages of droplet generation in the squeezing regime: **a** filling stage, the dispersed phase enters the outlet. P1 is the initial part of the filling stage in which the meniscus expands and the drop size is constant. P2 is the latter stage in which the meniscus recedes and the drop size increases; **b** necking, the dispersed thread rapidly decreases in diameter; **c** pinch-off, the thread collapses and a droplet separates from the bulk fluid at the junction



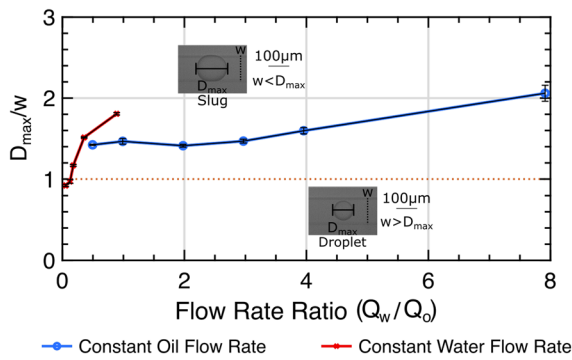


Fig. 4 Average non-dimensional drop size, $\frac{D_{max}}{w}$, vs the flow rate ratio, Q_w/Q_o . D_{max} is the average maximum diameter of the drop for slugs and drops, as shown in the image overlays

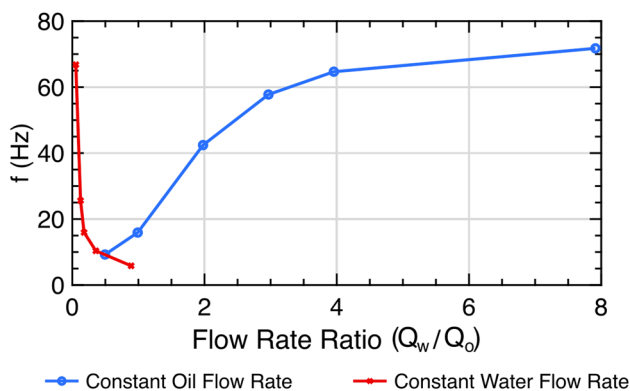


Fig. 5 Average drop generation frequency, f , vs flow rate ratio, Q_w/Q_o

increasing the generation frequency with a constant continuous flow rate.

To generate smaller drops, a separate set of experiments was performed in which the flow rate of the oil phase was varied for a constant, low water phase flow rate. Increasing the flow rate of the oil phase decreases the flow rate ratio and improves the pinch-off rate. This results in the production of smaller droplets at a higher frequency for a constant water phase flow rate, as shown in Figs. 4 and 5. This is due to an increase in the viscous shearing of the drop; however, as the flow rate ratio becomes smaller, drop size becomes less influenced by further increasing the oil phase flow rate, as shown in Fig. 4. Similar observations were made by Tan et al. (2006), who developed a power scaling law that showed a weak dependence of droplet size on the flow rate of the continuous phase for low flow rate ratios using similar geometry.

As the flow rate of the continuous fluid increases, the continuous phase velocity also increases and there is a corresponding increase in the pressure (Nisisako et al. 2002). As such, the pressure at high flow rates becomes a limiting factor for reducing droplet size. Ultimately, this pressure is

also influenced by other experimental parameters such as channel geometry and fluid viscosity. Chen et al. found that the pressure drop within the channel is related to geometrical parameters within the channel, as well as the Darcy friction factor which can be related to the fluid viscosity (Chen et al. 2011).

It is clear based in Fig. 2 that the addition of the orifice in the channel, when compared to van Loo’s observations, delays the jetting regime and expands the region in which squeezing occurs. This allows for the use of higher flow rates to generate droplets that are of high monodispersity, as shown Fig. 4. Furthermore, drop frequency is dependent upon the continuous oil and dispersed water phase flow rate, whereas drop size is primarily dependent upon the continuous oil phase flow rate.

3.2 Droplet generation in hydrophilic channels

In this section, we show that in the hydrophilic case, droplets form following the formation of single and double T-junctions which have not been reported by any other researchers. Figures showing the drop size and frequency, such as those shown in Figs. 4 and 5, were not possible for the hydrophilic channels, as the slugs and larger drops produced are sheared during flow through the outlet, causing the formation of secondary drops, found in Fig. 8a, which results in inconsistent drop sizes. Furthermore, high flow rates must be used to form smaller droplets that are not sheared by the walls; however, increasing the flow rate to these ranges results in high shear that strips the channel coating over time and results in repeatability discrepancies for drop size and frequency in these higher flow rate ranges.

3.2.1 Formation of a single T-junction

In the case of an applied hydrophilic coating, an inverse emulsion is obtained, where drops of oil are generated instead of DI water. Thus, in the hydrophilic channel, the dispersed phase is the silicone oil and the continuous phase is DI water. A notable aspect of the hydrophilic FF device is the formation of a single T-junction (STJ), as shown in Fig. 6. The expectation is that there will be two streams of oil from either side of the orifice. Instead, the fluid interface enters the junction and causes the oil phase to recede from the orifice, as shown in Fig. 6a, b. Upon reaching the orifice, (Fig. 6c), the interface grows until eventually rupturing, causing the water phase to flow out of the junction through the orifice outlet and an oil inlet, as shown in Fig. 6d.

This interface forms as a result of a non-uniformity of the contact angle in the hydrophilic channel. Due to this non-uniformity, during the formation of the single T-junction, asymmetry arises in the shape of the oil–water interface, as can be seen in Fig. 6c. This asymmetry results in the lower

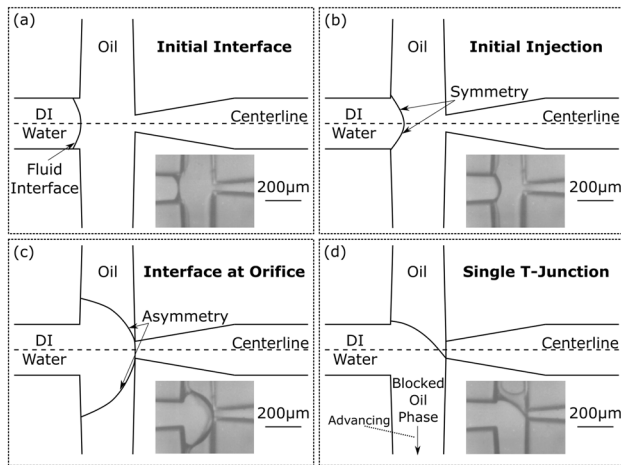


Fig. 6 Formation of the single T-junction ($\phi = 1$; $Ca_w = 4.3 \times 10^{-7}$); **a** fluid interface prior to the continuous phase injection into the junction and dispersed phase (silicone oil); **b** initial fluid interface after continuous phase injection into the junction; **c** fluid interface prior to reaching the orifice; **d** fluid interface after the continuous phase enters the orifice

side of the interface to reach the orifice wall before the top side. Once the interface grows and ruptures, the water phase wets the walls. The water phase has a smaller contact angle on the lower oil inlet walls than on the top oil inlet walls. When the meniscus ruptures, it wets the bottom wall, and allows the water phase to advance on the lower channel, causing the oil phase in the lower channel to recede. The bottom interface does not return to the junction and leads to an artificial ‘blockage’ of one of the dispersed oil phase inlets.

The curvature of this ‘blocked’ interface oscillates during slug generation in the squeezing regime, but ultimately, this interface oscillates about a fixed position for a given flow rate. Increasing the continuous phase flow rate shifts the position of this oscillation point further from the junction.

Due to the low viscosity of DI water, the viscous shearing of drops requires larger flow rates when compared to the hydrophobic channel. For a low continuous water phase capillary number, Ca_w , such as the one shown in Fig. 7a, the STJ forms slugs. As Ca_w increases, these slugs become smaller until they become oil droplets due to increase in viscous shearing. Further increase in Ca_w results in jetting for which the fluid interface no longer has the lag time associated with squeezing. These drops have diameters that are in the order of the orifice width. Figure 7b shows the jetting regime for the STJ. Similar to the hydrophobic channel, jetting is associated with rapid droplet formation. To verify the stability of the STJ, experiments were repeated and performed for an hour; however, the ‘blocked’ channel did not advance to the junction. In certain instances, the blocked channel changed sides. As such, it is assumed that the addition of the hydrophilic and partially oleophilic channel coating results

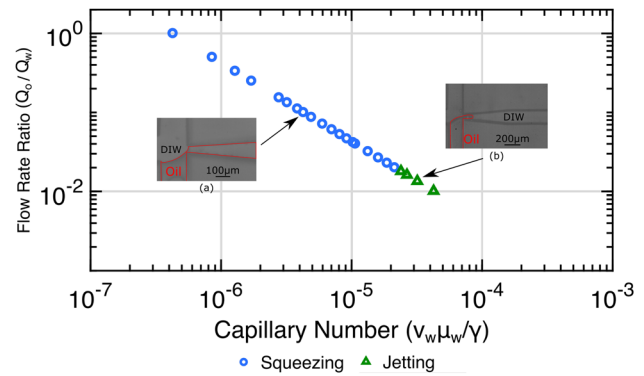


Fig. 7 Characteristic flow regimes for the hydrophilic channel with single T-junction (STJ) interface: **a** squeezing; **b** jetting. Fluid interface is artificially outlined to improve visualization

in a pressure metastability that restricts flow from entering a dispersed oil phase inlet.

The squeezing regime for the hydrophilic channel is shown in Fig. 8. During the filling stage, the dispersed oil phase enters the orifice and the drop size increases. As the drop grows larger, it coalesces with secondary oil droplets that are adhered to the wall. As the drop grows during the filling stage, necking occurs simultaneously and the fluid interface approaches the orifice corner of the unblocked oil inlet until pinch-off, as shown in Fig. 8b. As the slugs pinch-off and move along the channel, the wall shears the dispersed oil phase, shown in Fig. 8c, and produces small droplets that adhere to the wall, as shown in Fig. 8a. These secondary droplets are due to the partial wetting of the oil phase caused by the hydrophilic coating. Increasing the aqueous flow rate reduces the size and frequency of these adhered secondary droplets. This adhesion is similar to the results found by Dreyfus et al. when partial wetting was induced through the use of surfactants; however, their study found that stable droplet generation could not occur.

3.2.2 Formation of a double T-junction

A drawback of using a hydrophilic coating on the PDMS channel is that the coating strips off from some parts of the walls. This is due to the use of high flow rates within the hydrophilic coated channel, resulting in high shear stresses that remove parts of the coating from the wall as the coating is not a permanent one. This characteristic is consistent with a study by Roberts (2012). As a result, the channels become more hydrophobic and leads to a variation in the interface that makes it return to its hydrophobic characteristic. Thus, the artificial blockage produced when the channel is initially completely hydrophilic is removed, allowing for both dispersed phase inlets to reach the junction. This interface

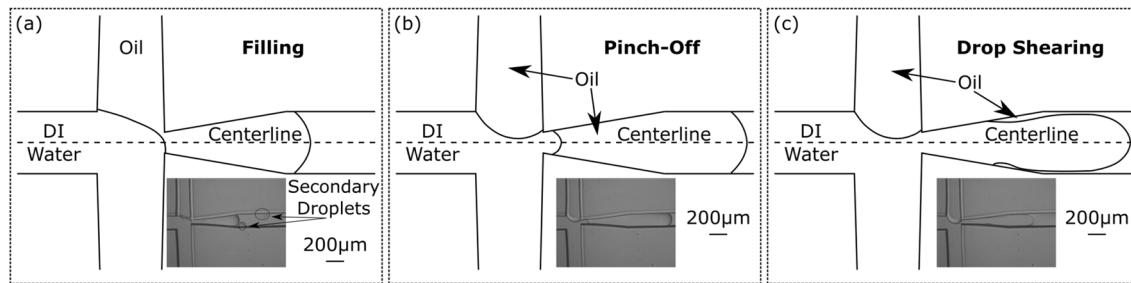


Fig. 8 STJ squeezing schematic for the hydrophilic channels. **a** Filling stage; **b** interface after the pinch-off of the oil droplet; **c** shearing of the oil phase results in the formation of secondary droplets shown in Fig. 2a

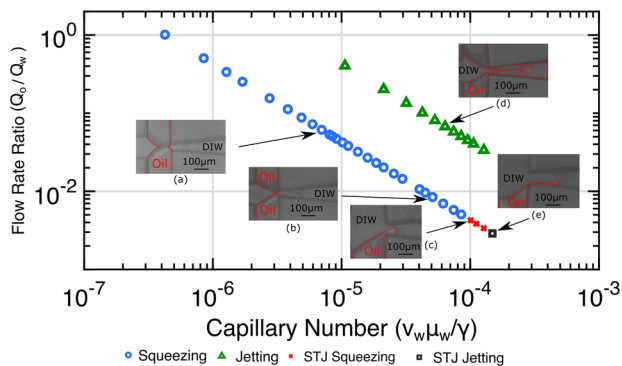


Fig. 9 Characteristic flow regimes for the hydrophilic channel with double T-junction (DTJ) interface. **a** Low capillary number squeezing; **b** high capillary number squeezing; **c** jetting/parallel flow; **d** STJ jetting. This interface is artificially outline to improve visualization

is referred to as the double T-junction (DTJ) and is shown in Fig. 9.

For low flow rate ratios, $\frac{Q_o}{Q_w}$, such as the one shown in Fig. 9a, the DTJ generates large slugs at the junction in the squeezing regime similar to the process shown in Fig. 8; however, both oil interfaces are at the junction. Initially, for low water capillary numbers, Ca_w , squeezing occurs for one oil interface, while the other interface is displaced away from the orifice by the incoming water phase. The inlet from which this drop forms varies between the oil inlets. Once the Ca_w is sufficiently large, both oil inlets produce drops in the squeezing regime.

During squeezing at low water capillary numbers, the dispersed oil phase restricts the continuous water phase from entering the orifice, resulting in a pressure build-up that causes intermittent slug formation. As the DI water flow rate increases, the viscous shearing imparted on the dispersed oil phase increases and prevents the constriction of the orifice, as shown in Fig. 9b. This eliminates the periodic pressure based squeezing in the low capillary region. Further increase in the water flow rate causes the slug generation rate to increase while decreasing the slug size. Once the water flow

rate, and consequently Ca_w , reaches a threshold value, the fluid interface changes once again to the STJ configuration as it originally did when the channel was completely coated with the hydrophilic material. It is conjectured that at these flow rates, pressure within the channel is sufficiently large and allows for the metastable structure to form once again.

At high capillary numbers, droplet generation occurs in the STJ squeezing regime, as shown in Fig. 9c. Comparing STJ squeezing for an initially completely coated channel with a partially coated channel shows that squeezing occurs at a larger Ca_w number and occurs where jetting would be expected. However, during each cycle of squeezing, two droplets are generated. Further increase in the water flow rate ultimately yields the STJ jetting regime, shown in Fig. 9e. Once droplet generation occurs, secondary droplets adhering to channel walls downstream are significantly reduced. Droplets have a diameter that is on the order of the orifice width and as a result, shearing of the dispersed phase at the walls is eliminated and secondary droplets are no longer prevalent as they were during slug formation.

Comparing the flow regimes observed in the hydrophobic channel, as shown in Fig. 2, with that observed in the hydrophilic channel, shown in Figs. 7 and 9, it can be seen that the capillary numbers obtained in the hydrophobic case are orders of magnitude larger. This is attributed to the change in the continuous fluid due to the variation in the contact angle within the channels. In the hydrophobic channel, oil is the continuous phase and has a larger viscosity than DI water. However, in hydrophilic channels, DI water becomes the continuous phase and has a lower viscosity. Results from these experiments show that under the same geometry and fluid inlet locations, a variation in the contact angle results in different flow regimes. For Figs. 7, 9 (flow rate ratio of 1 and Ca_w of 4.2×10^{-7}), and 2b, identical inlet flow rates are used; however, different flow regimes arise. The meniscus structure initially seen in the hydrophobic case in Fig. 3 disappears. The double T-junction case exhibits similar properties to both the hydrophobic and single T-junction case. For lower Ca_w values, and hence smaller DI water flow rates, both oil

inlet streams enter the junction, similar to the hydrophobic channel. For both cases, a large flow rate ratio and capillary number results in jetting, but these values are smaller in the hydrophilic case. For a constant oil phase flow rate, larger Ca_w in the double T-junction results in the formation of the single T-junction. It is hypothesized that the formation of the single T-junction is due to a pressure metastability within the channels, which can be explored in future studies.

4 Conclusion

The droplet generation process in two identical FF microchannels, with a diverging orifice design, is compared. One of the micro-channel is hydrophobic, whereas the other has a hydrophilic wall coating. It was found that for hydrophobic channels, the diverging orifice design delays jetting and expands the squeezing regime for drop generation compared to a symmetric microchannel with square cross junction. This allows for the use of higher flow rates to generate monodisperse droplets in the squeezing regime when compared with a symmetric cross-junction. The drop sizes from these experiments vary from 0.5 nl for the hydrophobic case to 0.15 ml in the hydrophilic case.

Coating the PDMS channels with a hydrophilic material resulted in an inverse emulsion and a variation of the fluid interface. Double T-junction and single T-junction structures developed during drop generation in this case. The single T-junction interface occurs initially when the channel walls are completely coated. Over time, this coating gradually wears away and results in the formation of the double T-junction interface. The formation of the single T-junction and double T-junction is conjectured to occur due to a pressure meta-stability within the hydrophilic, FF device. Partial wetting of the channel walls by the oil and water phase results in secondary droplets that adhere to the channel walls. These secondary droplets diminish with increase in the continuous water phase flow rate. While partial wetting of the channel walls by the dispersed oil phase occurred, stable droplet generation was achieved through the use of a chemical coating rather than surfactants to change the wetting property.

Results obtained from this study can be used to manipulate channel properties such that the diffusion of material into channel walls is minimized and to improve microfluidic device effectiveness. By further understanding the wetting properties and how the channel walls influence the flow structures and droplet generation, it will be possible to design and fabricate improved droplet devices.

References

- Abate AR et al (2009) Impact of inlet channel geometry on microfluidic drop formation. *Phys Rev E* 80(2):026310
- Anna SL, Bontoux N, Stone HA (2003) Formation of dispersions using flow focusing in microchannels. *Appl Phys Lett* 82(3):364–366
- Chan HF, Zhang Y, Leong KW (2016) Efficient one-step production of microencapsulated hepatocyte spheroids with enhanced functions. *Small* 12(20):2720–2730
- Chen JM, Kuo M-C, Liu C-P (2011) Control of droplet generation in flow-focusing microfluidic device with a converging-diverging nozzle-shaped section. *Jpn J Appl Phys* 50(10R):107301
- Chiu Y-L et al (2014) Synthesis of fluorosurfactants for emulsion-based biological applications. *ACS Nano* 8(4):3913–3920
- Cramer C, Fischer P, Windhab EJ (2004) Drop formation in a co-flowing ambient fluid. *Chem Eng Sci* 59(15):3045–3058
- Derzsi L et al (2013) Flow focusing with viscoelastic liquids. *Phys Fluids* 25(9):092001
- Dreyfus R, Tabeling P, Willaime H (2003) Ordered and disordered patterns in two-phase flows in microchannels. *Phys Rev Lett* 90(14):144505
- Edd JF et al (2008) Controlled encapsulation of single-cells into monodisperse picolitre drops. *Lab Chip* 8(8):1262–1264
- Fu T et al (2012) Droplet formation and breakup dynamics in microfluidic flow-focusing devices: from dripping to jetting. *Chem Eng Sci* 84:207–217
- Garstecki P et al (2004) Formation of monodisperse bubbles in a microfluidic flow-focusing device. *Appl Phys Lett* 85(13):2649–2651
- Glawdel T, Elbuken C, Ren CL (2012) Droplet formation in microfluidic T-junction generators operating in the transitional regime. II. Modeling. *Phys Rev E* 85(1):016323
- Gu H, Duits MHG, Mugele F (2011) Droplets formation and merging in two-phase flow microfluidics. *Int J Mol Sci* 12(4):2572–2597
- Gupta A, Kumar R (2010) Droplets formation and merging in two-phase flow microfluidics. *Microfluid Nanofluid* 8(6):799–812
- Gupta A, Matharoo HS et al (2014) Droplet formation via squeezing mechanism in a microfluidic flow-focusing device. *Comput Fluids* 100:218–226
- Gupta A, Sohel Murshed SM, Kumar R (2009) Droplet formation and stability of flows in a microfluidic T-junction. *Appl Phys Lett* 94(16):164107
- Kaler KVIS, Prakash R (2014) Droplet microfluidics for chip-based diagnostics. *Sensors* 14(12):23283–23306
- Kim TJ, Hidrovo C (2012) Pressure and partial wetting effects on superhydrophobic friction reduction in microchannel flow. *Phys Fluids* 24(11):112003
- McClements DJ, Decker EA (2000) Lipid oxidation in oil-in-water emulsions: impact of molecular environment on chemical reactions in heterogeneous food systems. *J Food Sci* 65(8):1270–1282
- Mehta G et al (2012) Opportunities and challenges for use of tumor spheroids as models to test drug delivery and efficacy. *J Control Release* 164(2):192–204
- Nie Z et al (2008) Emulsification in a microfluidic flow-focusing device: effect of the viscosities of the liquids. *Microfluid Nanofluid* 5(5):585–594
- Nisisako T, Torii T, Higuchi T (2002) Droplet formation in a microchannel network. *Lab Chip* 2(1):24–26
- Nooranidoost M et al (2019) Cell encapsulation modes in a flow-focusing microchannel: effects of shell fluid viscosity. *Microfluid Nanofluid* 23(3):31
- Roberts CC et al (2012) Comparison of monodisperse droplet generation in flow-focusing devices with hydrophilic and hydrophobic surfaces. *Lab Chip* 12(8):1540–1547

- Serra C et al (2007) A predictive approach of the influence of the operating parameters on the size of polymer particles synthesized in a simplified microfluidic system. *Langmuir* 23(14):7745–7750
- Srinivasan V, Pamula VK, Fair RB (2004) An integrated digital microfluidic lab-on-a-chip for clinical diagnostics on human physiological fluids. *Lab Chip* 4(4):310–315
- Takeuchi S et al (2005) An axisymmetric flow-focusing microfluidic device. *Adv Mater* 17(8):1067–1072
- Tan Y-C, Cristini V, Lee AP (2006) Monodispersed microfluidic droplet generation by shear focusing microfluidic device. *Sens Actuators B Chem* 114(1):350–356
- Teo AJT, Tan SH, Nguyen N-T (2019) On-demand droplet merging with an AC electric field for multiple-volume droplet generation. *Anal Chem* 92(1):1147–1153
- Tice JD et al (2003) Formation of droplets and mixing in multiphase microfluidics at low values of the Reynolds and the capillary numbers. *Langmuir* 19(22):9127–9133
- Tomasz G, Carolyn RL (2012) Droplet formation in microfluidic T-junction generators operating in the transitional regime. III. Dynamic surfactant effects. *Phys Rev E* 86(2):026308
- Utada AS et al (2007) Dripping to jetting transitions in co-flowing liquid streams. *Phys Rev Lett* 99(9):094502
- Van Loo S et al (2016) Droplet formation by squeezing in a microfluidic cross-junction. *Microfluid Nanofluid* 20(10):146
- van Steijn V, Kreutzer MT, Kleijn CR (2007) μ -PIV study of the formation of segmented flow in microfluidic T-junctions. *Chem Eng Sci* 62(24):7505–7514
- Wang L et al (2007) Oil-in-water nanoemulsions for pesticide formulations. *J Colloid Interface Sci* 314(1):230–235
- Wehking JD et al (2014) Effects of viscosity, interfacial tension, and flow geometry on droplet formation in a microfluidic T-junction. *Microfluid Nanofluid* 16(3):441–453
- Woolford B, Maynes D, Webb BW (2009) Liquid flow through microchannels with grooved walls under wetting and superhydrophobic conditions. *Microfluid Nanofluid* 7(1):121–135
- Yakhshi-Tafti E, Kumar R, Cho HJ (2011) Measurement of surface interfacial tension as a function of temperature using pendant drop images. *Int J Optomechatron* 5(4):393–403
- Yobas L et al (2006) High-performance flow-focusing geometry for spontaneous generation of monodispersed droplets. *Lab Chip* 6(8):1073–1079
- Zhang Y et al (2013) A programmable microenvironment for cellular studies via microfluidics-generated double emulsions. *Biomaterials* 34(19):4564–4572
- Zhao C-X (2013) Multiphase flow microfluidics for the production of single or multiple emulsions for drug delivery. *Adv Drug Deliv Rev* 65(11–12):1420–1446
- Zhu P, Wang L (2017) Passive and active droplet generation with microfluidics: a review. *Lab Chip* 17(1):34–75

Publisher's Note Springer Nature remains neutral with regard to jurisdictional claims in published maps and institutional affiliations.